Modification by protons of frog skeletal muscle K_{ATP} channels: effects on ion conduction and nucleotide inhibition

Michel Vivaudou and Cyrille Forestier

CEA, DBMS, Biophysique Moléculaire et Cellulaire (URA CNRS 520), 17 rue des Martyrs, 38054 Grenoble, France

1. The molecular mechanisms underlying pH regulation of skeletal muscle ATP-sensitive K^+ (K_{ATP}) channels were studied using the patch clamp technique in the inside-out configuration. Two effects of intracellular protons were studied in detail: the decrease in magnitude of single-channel currents and the increase in open probability (P_o) of nucleotide-inhibited channels.

2. The pH dependence of inward unit currents under different ionic conditions was in poor agreement with either a direct block of the pore by protons or an indirect proton-induced conformational change, but was compatible with the protonation of surface charges located near the cytoplasmic entrance of the pore. This latter electrostatic mechanism was modelled using Gouy–Chapman–Stern theory, which predicted the data accurately with a surface charge density of about 0·1 negative elementary charges per square nanometre and a pK (pH value for 50% effect) value for protonation of these charges of 6·25. The same mechanism, i.e. neutralization of negative surface charges by cation binding, could also account for the previously reported reduction of inward unit currents by Mg^{2+}.

3. Intracellular alkalization did not affect P_o of the K_{ATP} channels. Acidification increased P_o. In the presence of 0·1 mM ATP (no Mg^{2+}), the channel activation *vs.* pH relationship could be fitted with a sigmoid curve with a Hill coefficient slightly above 2 and a pK value of 6. This latter value was dependent on the ATP concentration, decreasing from 6·3 in 30 μM ATP to 5·3 in 1 mM ATP.

4. Conversely, the channel inhibition *vs.* ATP concentration curve was shifted to the right when the pH was lowered. At pH 7·1, the ATP concentration causing half-maximal inhibition was about 10 μM. At pH 5·4, it was about 400 μM. The Hill coefficient values remained slightly below 2. Similar effects were observed when ADP was used as the inhibitory nucleotide.

5. These results confirm that a reciprocal competitive link exists between proton and nucleotide binding sites. Quantitatively, they are in full agreement with a steady-state model of a K_{ATP} channel possessing four identical protonation sites (microscopic pK, 6) allosterically connected to the channel open state and two identical nucleotide sites (microscopic ATP dissociation constant, ~30 μM) connected to the closed state.

Potassium-selective channels inhibited by intracellular ATP (K_{ATP} channels) have been found in many tissues, including most types of muscle (Ashcroft & Ashcroft, 1990). As other channels like voltage-dependent Na^+, K^+ and Ca^{2+} channels serve to transmit membrane electrical excitation and couple it to metabolic processes, K_{ATP} channels could provide a sort of feedback control by linking excitability to cellular energy levels. In skeletal muscle, this hypothesis is strengthened by the observation that K_{ATP} channels are regulated not only by ATP, which alone is a poor metabolic index, but also by ADP and pH. ADP may cause channel activation by both competitive relief of ATP inhibition (Vivaudou, Arnoult & Villaz, 1991) and ATP-independent, possibly Mg^{2+}-dependent, interaction (Allard & Lazdunski, 1992; Forestier & Vivaudou, 1993*a*). Protons, at micromolar concentrations, are also potent activators of skeletal muscle K_{ATP} channels (Davies, 1990) and they appear to act mainly by competitively decreasing channel sensitivity to ATP inhibition (Davies, Standen & Stanfield, 1992). The same group also reported that protons decreased outward single-channel currents.

In this work, we have examined in further detail the effects of intracellular protons on the permeation properties and steady-state nucleotide dependence of skeletal muscle K_{ATP}

channels. Extensive quantitative data are presented on proton-induced changes in inward unit currents and on the functional interaction between protons and the nucleotides ATP and ADP.

The conductance data were found to be most consistent with an electrostatic mechanism, whereby negative surface charges would exist at the cytoplasmic entrance of the channel and neutralization of these charges by protonation would reduce local surface potentials, 'tilt' the pore electrical field and therefore reduce ion flux (Mackinnon, Latorre & Miller, 1989).

The open probability (P_o) data corroborate the existence of a competitive connection between proton and ATP/ADP binding sites. Protons decreased the sensitivity to ATP or ADP inhibition and, reciprocally, ATP decreased the sensitivity to proton activation. The pK (pH value for 50% effect) of the proton activation effect was therefore not constant but changed with the concentration of ATP present. The full set of experimental data could be reconstructed using an allosteric model in which the channel is stabilized in an open state upon occupancy of one of four identical protonation sites or in a closed state upon occupancy of one of two nucleotide binding sites.

A preliminary report of some of the results presented here has been published in abstract form (Forestier & Vivaudou, 1993*b*).

METHODS

Experimental set-up

Using the patch clamp technique (Hamill, Marty, Neher, Sakmann & Sigworth, 1981) single-channel currents were recorded in inside-out patches excised from the membrane of split-fibre blebs. Formation of these large sarcolemmal blebs was induced by mechanical cleavage of fibres dissected from the iliofibularis of the frog, *Rana esculenta* (killed by decapitation), as described previously (Vivaudou *et al.* 1991).

Patch pipettes (resistance, 3–20 MΩ) were pulled from borosilicate capillaries (Kimax-51 34502, T & M, BP52, 94403, Vitry-sur-Seine, France) on a BB-CH horizontal puller (Mechanex, Nyon, Switzerland). Currents were measured using a Bio-Logic RK-300 amplifier (Bio-Logic, Claix, France), filtered at a cut-off frequency of 0·3 kHz and stored on digital audio tapes, together with either membrane voltage or a solution identification signal. Unless otherwise specified, the membrane potential (V_m) was −50 mV.

Application of the various solutions to the intracellular side of the patch was performed using a Bio-Logic RSC-100 rapid solution changer which is an improved version of the 'sewer pipes' system introduced by Yellen (1982). This device was operated by the custom software Perf 2.10, (M. Vivaudou, available on request) which permits the application of combined voltage and perfusion protocols of any complexity. Tube switching duration was routinely set at 50 ms. However, full solution exchange at the intracellular face of the patch could be considerably longer depending on how fast the solutions flowed out of the tubes and how far the patch of membrane was from the pipette tip (Cannell & Nichols, 1991).

The conclusions presented here are a synthesis of data gathered from more than 100 patches. Numerical results are presented as means ± S.D. (n indicates sample size).

Solutions

Solutions were designed to optimize recording of K_{ATP} channels and minimize contamination by other channels. The patch pipette contained 150 mM K^+, 136 mM Cl^-, 2 mM Mg^{2+} and 10 mM Pipes. The cytoplasmic face of the patch was bathed in solutions which all contained 150 mM K^+, 40 mM Cl^-, 1 mM EGTA, 10 mM Pipes and methanesulphonate ions as the remaining anions except for the K^+-free solutions which contained various concentrations of ATP, 40 mM Na^+, 30 mM Cl^-, 1 mM EGTA, 10 mM Pipes and 200 mM saccharose to maintain equiosmolarity. Unless expressly indicated, solutions contained no added Mg^{2+}.

Solutions were titrated with KOH or HCl and their pH values were found to remain stable during the course of an experiment even when outside the effective buffering range of Pipes (i.e. pH 5·8–7·8). When not explicitly specified, the pH was set to 7·1. Experiments were conducted at room temperature (22–24 °C). ATP (sodium salt for K^+-free solutions and potassium salt otherwise) was purchased from Sigma.

Data acquisition

Stored signals were sampled (1–10 kHz) and processed with an IBM-compatible microcomputer. For presentation of long stretches of data, appropriate Gaussian filtering and undersampling were done numerically. Final cut-off and sampling frequencies are indicated in the figures as f_c and f_s, respectively. Slow fluctuations of the no-channel-open baseline of the current signal were removed by interactive fitting of the baseline with a spline curve and subtraction of this fit from the signal. Acquisition, analysis and presentation were performed using the custom software Erwin 3.1 (M. Vivaudou, available on request). Curve fitting was done using MicroCal Origin 3.5 (non-linear regression by the Levenberg–Marquardt method). Mathematical modelling and iterative solving of complex equations were done using MathCad 4.0 (Mathsoft Inc., Cambridge, MA, USA). Final figures were drawn using Corel Draw 5.0.

Unitary currents were estimated by selecting well-defined opening and closing transitions and measuring the magnitude of the corresponding current steps with horizontal cursors. This method is faster than measuring the distances separating the peaks of amplitude histograms. It is also probably more accurate since cursor measurements are obtained from only long clear openings which are less subject to attenuation by filtering.

Mean patch current (I) was computed by averaging data points over portions of the signal delimited by cursors. The number of active channels (N) in a patch was often large and difficult to estimate with accuracy. Since $I = NP_o i$, mean current was used to track change in channel open probability (P_o) under conditions in which the single-channel unit current (i) stayed constant. As demonstrated below, unit current varies with pH. Therefore, in those experiments in which channel activities at different pH values needed to be compared, we used the quantity I/i (i.e. NP_o) as an indicator proportional to P_o. Values of i at different pH values were taken from the data presented in the first part of the Results section.

Note that the use of I or NP_o as an indicator of channel activity is valid only if N does not change. It is well known that K_{ATP} channels are subject to run-down, i.e. a time-dependent decrease in N. In our preparation, the rate of run-down usually stayed

below 1–10% min^{-1} and had little influence on our results since sets of related data, such as all points of a dose–response curve, could be collected within a minute or so. Nonetheless, the extent of run-down during an experiment was always verified by measuring maximum channel activity at regular intervals and measurements were corrected assuming a linear decrease in channel number during those intervals.

Nucleotide dose responses

A nucleotide dose–response run consisted of recording mean current over a full range of nucleotide concentrations at a given pH. In a single patch, several such runs could be performed and repeated at two or more pH values. For each of these runs, the data points were plotted as mean current *vs.* nucleotide concentration and fitted to the following standard Hill function for a full inhibitor:

$$I([\text{nucleotide}]) = \frac{I_{max}}{1 + \left[\frac{[\text{nucleotide}]}{K_{½}}\right]^{n}}, \quad (1)$$

in order to determine: I_{max}, the current expected in absence of nucleotide; $K_{½}$, the concentration causing 50% inhibition; and n, the Hill coefficient. Note that I_{max} is a best estimate based on all data points whereas the current actually measured in the absence of nucleotide constitutes a single data point. Both values need not be the same but were close in practice. In the patches considered for analysis, channels were nearly fully open in the absence of nucleotide ($P_o = 1$) and fully closed at high nucleotide concentrations ($P_o = 0$). Therefore, experimental mean current values could be transformed into P_o values by dividing them by I_{max}. Thus, each dose–response run yielded a set of P_o values, which were then all pooled and averaged. These average values were plotted and could be fitted to eqn (1) to obtain values of $K_{½}$ and the Hill coefficient of the average response of all patches.

Proton dose responses

In each patch, mean current (I(pH)) was measured over a range of pH values. NP_o(pH) was derived from the ratio of the measured mean current and the unit current at that pH as discussed above. Since little activation was observed at pH values above 7 (see Results), control activity, theoretically in the absence of protons, was taken as the activity recorded at the highest pH tested, usually pH 7·8 or 7·1. Proton-induced activity was therefore evaluated as NP_o(pH) − NP_o(pH > 7).

Using the classical formulation for agonist–receptor interaction, this proton-induced activity (A) was analysed in terms of a Hill relation:

$$A(\text{pH}) = \frac{A_{max}}{1 + 10^{n(\text{pH} - \text{p}K)}}, \quad (2)$$

where A_{max} is the theoretical maximum activity, n is the dimensionless Hill coefficient and pK is the pH value causing 50% activation. The fit of the data points to this function yielded a value of A_{max} which by division was used to transform the measurements into normalized proton-induced activity. This quantity is equivalent to the fractional increase, ΔP_o(H), of the open probability caused by a concentration, H, of protons. For each patch where full dose–response was available, this procedure supplied a set of ΔP_o values as well as values of pK and the Hill coefficient which described the dependence on pH of the individual patch. The ΔP_o values were averaged, plotted and could be fitted to eqn (2) to obtain pK and Hill coefficient values of the average response of all patches.

RESULTS

Protons and ion conduction through K_{ATP} channels

Inward rectification properties of K_{ATP} channels are well known and can be explained partly by a voltage-dependent block by intracellular cations such as Mg^{2+} or Na^+ (Findlay, 1987; Horie, Irisawa & Noma, 1987; Vivaudou *et al.* 1991). The reduction in outward current through K_{ATP} channels by protons observed in skeletal muscle fibres (Davies *et al.* 1992), cardiac myocytes (Cuevas, Bassett, Cameron, Furukawa, Myerburg & Kimura, 1991; Koyano, Kakei, Nakashima, Yoshinaga, Matsuoka & Tanaka, 1993) and pancreatic β-cells (Proks, Takano & Ashcroft, 1994) could be attributed to a similar mechanism involving a rapid block by protons. However, it could also partly arise from cancellation of negative surface charges which normally boost K^+ flux by attracting intracellular K^+ ions into the cytoplasmic vestibule of the pore.

Here, we have focused on inward rather than outward currents since acidification also reduces inward currents, as

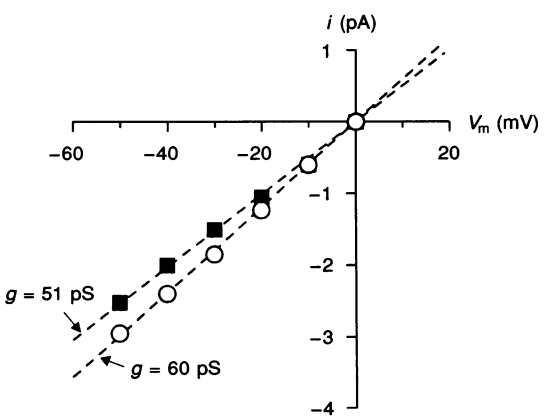

Figure 1. Intracellular acidification attenuates inward unit currents

Plot of channel unitary current *vs.* voltage at pH 7·1 (○) and 5·4 (■). Dashed lines are best fits to Ohm's law and yield conductances (g) of 60 (pH 7·1) and 51 (pH 5·4) pS. Standard Mg^{2+}-free solutions with 100 μM (pH 7·1) and 1 mM (pH 5·4) intracellular ATP were used. Patch no. 432305.

shown in heart (Cuevas *et al.* 1991; Fan, Furukawa, Sawanobori, Makielski & Hiraoka, 1993; Koyano *et al.* 1993) and in pancreas (Proks *et al.* 1994). We have also found this to be the case in skeletal muscle. Under conditions of normal ionic strength and symmetrical K^+, acidification caused an apparent reduction in conductance (Fig. 1).

Inward current reduction is not easily explained by protons entering and blocking the channel conduction pathway since one would expect that the block would be relieved as potentials become more negative. Alternatively, an electrostatic effect mediated by alterations in negative surface charge could be postulated. Indeed intracellular protons decrease the inward current through K_{ATP} channels in much the same way as chemical removal of extracellular negatively charged groups decreases the outward current through K_{Ca} channels (Mackinnon *et al.* 1989).

Intracellular negative surface charges near the pore entrance may affect cation conduction in two opposite ways. First, they attract cations thus raising the local permeant ion concentrations. The resulting change of the local chemical gradient favours outward cation flux. Second, they give rise to a negative surface potential which will pull in extracellular cations through the pore by augmenting the voltage drop across the channel conduction pathway. This 'tilt' of the energy profile (Mackinnon *et al.* 1989) favours inward cation flux. In symmetrical K^+ as in Fig. 1, if protons affect surface charge, the observed changes in unit current should depend on how protons alter the balance between these two antagonistic mechanisms at each applied voltage. With intracellular solutions devoid of permeant ions only the 'tilt' effect should be observed. Figure 2 illustrates the pH dependence of current–voltage curves obtained with such a solution. It can be seen that protons preserve the shape of the current–voltage curve while translating it towards more negative potentials. This is what would be expected if protons cancelled negative charges near the cytoplasmic entrance of the pore, thus removing the voltage offset arising from those charges. Our experimental results on the effects of protons on K_{ATP} single-channel currents are summarized in Fig. 3*A*. The inward single-channel current at −50 mV was measured at different pH values in either normal 150 mM K^+ solution or K^+-free solution. For each patch, normalized values of current, $i_{norm}(H)$, were obtained by dividing the current at a given proton concentration, $i(H)$, by the current at

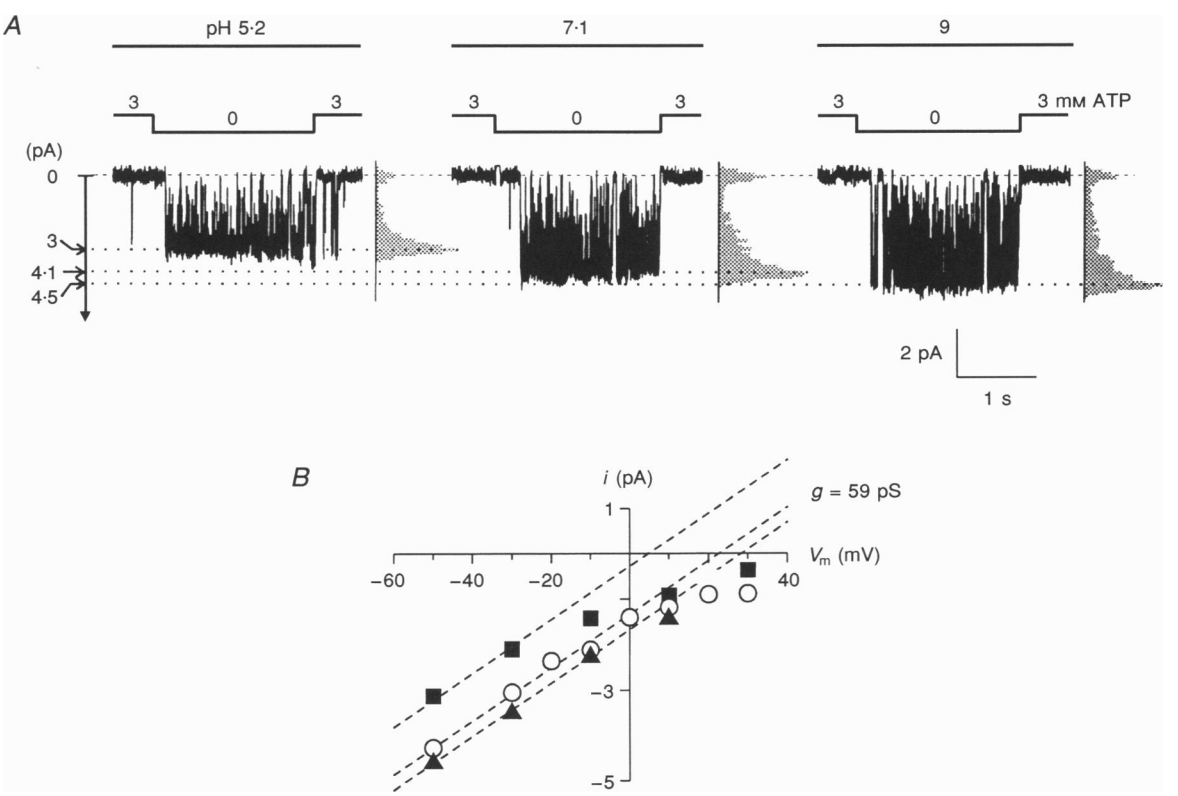

Figure 2. In the absence of permeant ions, intracellular acidification shifts the unitary current *vs.* voltage plot along the voltage axis

A, opening of a single K_{ATP} channel upon removal of ATP at acidic, normal and basic pH. Traces were recorded at 4 s intervals in the order shown. Amplitude histograms of each trace segment are displayed to the right of each trace. Bin width, 120 fA; f_s, 1 kHz; f_c, 330 Hz. Patch no. 442810. *B*, plots of channel unitary current *vs.* voltage at pH 5·2 (■), 7·1 (○) and 9 (▲). Dashed lines have a slope (*g*) of 59 pS. Bath solutions: K^+-free solutions with 0 or 3 mM ATP.

pH 7·1. In symmetrical K^+ solutions, i_{norm} is maximal at basic pH and declines steadily at acidic pH. In K^+-free solution, these effects appeared larger.

We have tried to correlate the data of Fig. 3*A* with predictions based on models in which protons could either block conduction or cancel surface charges, or both. If protons simply blocked the pore with a dissociation constant, $K_{d,b}$, the inward current, $i(H)$, as a function of proton concentration, H, would follow the relation:

$$i(H) = \frac{i(0)}{1 + H/K_{d,b}}. \quad (3)$$

This model (dotted line in Fig. 3*A*) could not adequately account for the steep decline in current at low H^+ concentrations and the more sluggish decline at higher concentrations. We therefore investigated a model involving cancellation of negative surface charges by protons, which did produce a much better fit of the experimental data.

K_{ATP} channels have been shown to deviate somewhat from the constant-field theory (Spruce, Standen & Stanfield, 1987). Assuming that this deviation is small, at potentials sufficiently negative and in the presence of a high extracellular K^+ concentration ($[K^+]_o$), the inward K^+ current is expected to vary linearly with potential and independently of intracellular K^+ concentration ($[K^+]_i$) (Hille, 1992). This means that, as intracellular surface charges are cancelled, changes in local $[K^+]_i$ would not contribute significantly to the variations in inward current observed at −50 mV as in Fig. 3*A*. As a first approximation we therefore assumed that unitary currents at −50 mV were not significantly affected by local concentration changes and, in order to interpret our results, we used the following equation from Mackinnon *et al.* (1989), even though it was derived for cases where permeant ions are only on one side. Considering that protons can alter the driving force and block the channel, this equation relates inward current, $i(H)$, and proton concentration, H:

$$i(H) = \frac{i(0) + 10^{-3} g[\psi(0) - \psi(H)]}{1 + (H/K_{d,b})\exp(-\psi(H)/V)}, \quad (4)$$

where $i(H)$ is in picoamperes; g is the channel conductance in picosiemens; $\psi(H)$ is the local electrostatic potential at the cytoplasmic end of the pore in millivolts; and $K_{d,b}$ is the dissociation constant of pore blockade by protons. The factor V is 25 mV at room temperature. The local potential depends in a complex way on the configuration of surface charges and on the degree to which they are cancelled by ions in solution through screening or binding. Nonetheless, the problem can usually be simplified by assuming a uniform planar charge distribution. This assumption,

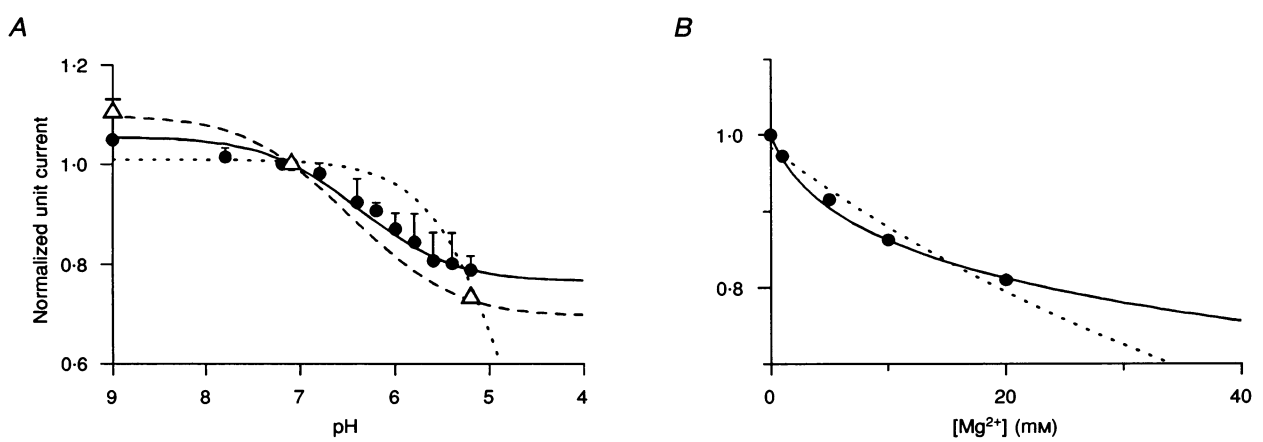

Figure 3. Proton and Mg^{2+} dependence of the inward single-channel current amplitude is more compatible with surface charge cancellation than with channel block

A, currents were measured at −50 mV at different pH values, normalized for each patch to the value measured at pH 7·1, and averaged over all patches. Bath solution was either normal 150 mM K^+ (●) or low ionic strength K^+ free (△). Each point with the associated error bar (when larger than symbol) is the mean ± S.D. of at least 3 values. The dotted line which is the best fit of the 150 mM K^+ data to eqn (3) represents the prediction of a bimolecular block model with $pK_{d,b}$ of 4·7. The continuous line corresponds to a Gouy–Chapman–Stern (GCS) model and is calculated from eqns (4) and (5) for the 150 mM K^+ bath solution with $i(0)$, 3·6 pA; g, 60 pS; σ, $9{\cdot}6 \times 10^{-2}$ charges nm^{-2}; $pK_{d,sc}$, 6·25; and $pK_{d,b}$, 0 (i.e. no proton block). The dashed line is the corresponding curve for the K^+-free solution with the same parameters except that $i(0)$ is 5 pA. *B*, currents were measured at −80 mV in the presence of different concentrations of intracellular Mg^{2+} (data from previous work, Forestier & Vivaudou, 1993*a*) and normalized to the value measured in the absence of Mg^{2+}. Bath solution was standard 150 mM K^+. The dotted line, predicted by a bimolecular block model, is the best fit of the data to the equivalent for Mg^{2+} of eqn (3) ($K_{d,b}$ = 84 mM). The continuous line, predicted by a GCS model, is calculated from eqns (6) and (7) with $i(0)$, 4 pA; g, 60 pS; σ, $9{\cdot}6 \times 10^{-2}$ charges nm^{-2}; $K_{d,sc}$, 30 mM; and $K_{d,b}$, 700 mM. Patch no. 19M2.

although obviously unjustified, sustains the Gouy–Chapman model which has been used extensively and found to be adequate in most cases (Mclaughlin, 1977). Since pH changes in the range 9–5 would not yield any significant change in ionic strength, one is obliged to postulate that protons neutralize surface charge primarily by binding to surface charges. We have therefore adopted a Gouy–Chapman–Stern type of model integrating screening and binding (Mclaughlin, Szabo & Eisenman, 1971; Wilson, Morimoto, Tsuda & Brown, 1983), which yields the following relationship between local potentials, surface charges and solution composition:

$$\frac{\sigma}{\left[1+\frac{H}{K_{d,sc}}\exp\left(-\frac{\psi(H)}{V}\right)\right]}=\frac{\sqrt{\sum_j C_j\left[\exp\left(\frac{-z_j\psi(H)}{V}\right)-1\right]}}{G}, \quad (5)$$

where σ is the surface charge density in nm^{-2} (number of negative elementary charges per unit area); C_j is the bulk concentration in moles per litre of ions of valence z_j in the intracellular solution; and factor G is 2·7 nm^2 $(mol\ l^{-1})^{½}$ at room temperature. Protons can bind to the surface charges with a dissociation constant, $K_{d,sc}$.

This model has three unknown parameters: the surface charge density σ and the dissociation constants $K_{d,sc}$ and $K_{d,b}$; and two parameters which may be evaluated experimentally: the control current $i(0)$ and the channel conductance g. Starting with reasonable guesses for these five parameters, eqn (5) was solved numerically to obtain estimates of the potential $\psi(H)$, which were then used to calculate $i(H)$ from eqn (4) and obtain $i_{norm}(H)$. The resulting curve was compared with the experimental data and the parameters were adjusted to improve the match. This process quickly revealed that the data could be modelled adequately without having to consider that protons blocked the pore (i.e. $K_{d,b}=\infty$ in the above equations), at least in the range of pH values tested. With a density of about 0·1 charges nm^{-2} and a binding constant corresponding to pH 6·25, the model accurately predicted the observed pH dependence of inward current under the two ionic conditions tested.

We have shown in a previous paper (Forestier & Vivaudou, 1993*a*) that Mg^{2+} at millimolar concentrations also reduced inward currents. If one assumes that Mg^{2+} can also neutralize surface charges by binding to divalent anionic

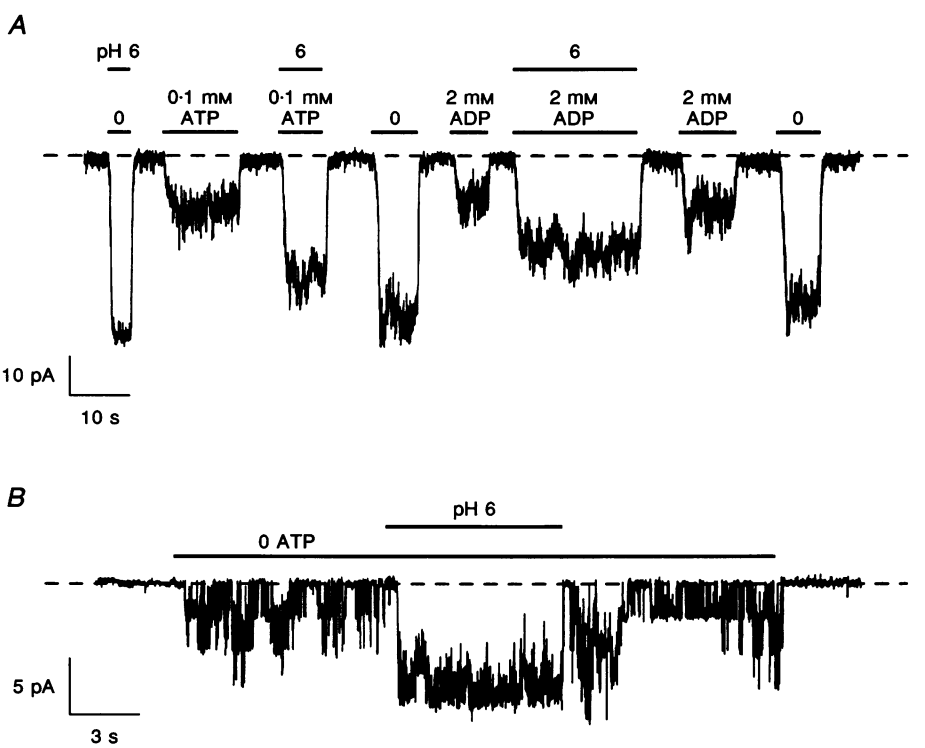

Figure 4. Activation by acidification with and without nucleotides

A, acidification activates K_{ATP} channels blocked by ADP as well as by ATP. The horizontal bars above the trace indicate the application of nucleotides at the concentrations shown (without Mg^{2+}; 0 indicates no nucleotide present; in the parts of the trace not covered by a bar a blocking solution of 3 mM ATP and 5 mM Mg^{2+} was applied) and the periods of acidification to pH 6 (pH 7·1 otherwise). f_s, 200 Hz; f_c, 60 Hz. Patch no. 292404. *B*, acidification can activate K_{ATP} channels in the absence of nucleotides. The patch was bathed in a '0 ATP' solution (containing 5 mM Mg^{2+}) or a blocking solution of 3 mM ATP and 5 mM Mg^{2+} and the pH was lowered from 7·1 to 6 as indicated. f_s, 500 Hz; f_c, 250 Hz. Patch no. 280404B.

sites, the following eqns, analogous to eqns (4) and (5), will apply:

$$I(\mathrm{Mg}) = \frac{i(0) + 10^{-3} g[\psi(0) - \psi(\mathrm{Mg})]}{1 + (\mathrm{Mg}/K_{d,b})\exp(-2\psi(\mathrm{Mg})/V)}, \quad (6)$$

and

$$\frac{\sigma}{\left[1 + \frac{\mathrm{Mg}}{K_{d,sc}}\exp\left(\frac{-2\psi(\mathrm{Mg})}{V}\right)\right]} = \frac{\sqrt{\sum_j C_j}\left[\exp\left(\frac{-z_j\psi(\mathrm{Mg})}{V}\right) - 1\right]}{G}, \quad (7)$$

where Mg denotes the concentration of Mg^{2+} in the bath. As shown in Fig. 3*B*, a good correlation between the measured and the computed inward currents was obtained with the same density of 0·1 charges nm^{-2}, a binding constant of 30 mM, and a rather weak block ($K_{d,b}$ = 700 mM). Note that if one assumes a 1:1 binding of Mg^{2+} and protons to the same monovalent charges, a slightly more complicated eqn than eqn (7) (see Mclaughlin, Mulrine, Gresalfi, Vaio & Mclaughlin, 1981) must be used but it yielded very similar values (same σ; $K_{d,sc}$ = 35 mM; $K_{d,b}$ = 330 mM).

Activation of K_{ATP} channels by protons

Under most conditions, acidification triggers a net, large increase in mean current because the single-channel current decrease is far outweighed by a significant increase in P_o (Davies *et al.* 1992). The second part of this work concerns this latter phenomenon.

K_{ATP} channels are inhibited in a dose-dependent manner by ATP. The concentration of ATP producing 50% inhibition, $K_{½}$, is variable from patch to patch and its range

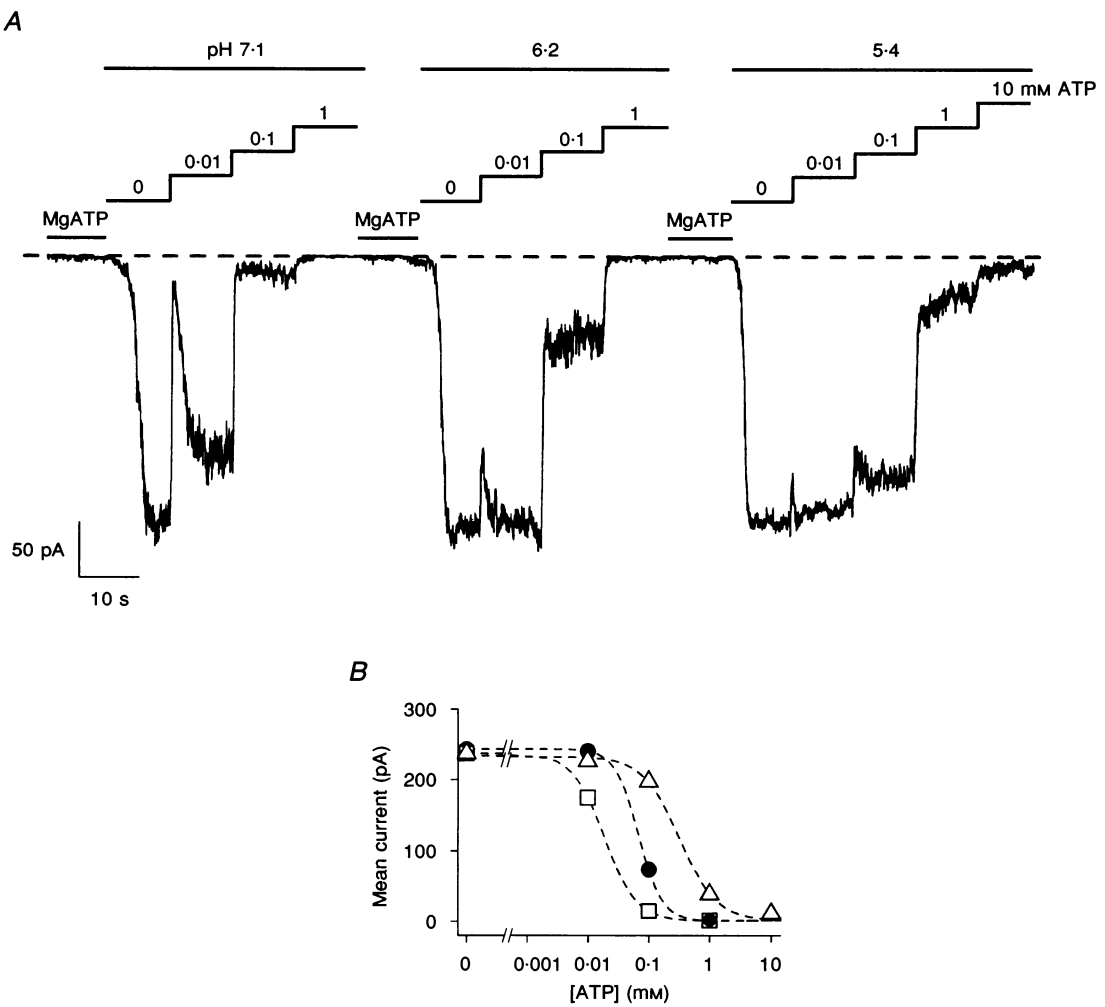

Figure 5. Acidic pH shifts the ATP dependence of K_{ATP} channels

A, currents recorded at increasing concentrations of ATP at neutral and acidic pH. The horizontal bars above the trace indicate the application of ATP at the concentrations shown (without Mg^{2+}) and the pH of the solutions. In between the dose responses, a blocking solution of 3 mM ATP and 5 mM Mg^{2+} (pH 7·1) was applied (horizontal bars marked MgATP). f_s, 125 Hz; f_c, 40 Hz. Patch no. 432301. *B*, corresponding plots of the measured mean current at each concentration of ATP *vs.* ATP concentration at pH 7·1 (□), 6·2 (●) and 5·4 (△). Dashed lines are best fits of the data points to eqn (1) with values of $K_{½}$ and the Hill coefficient, respectively, of 19 μM and 1·6 (pH 7·1), 69 μM and 2·2 (pH 6·2) and 325 μM and 1·4 (pH 5·4).

can span more than one order of magnitude under identical experimental conditions (Findlay & Faivre, 1991; Vivaudou *et al.* 1991). This unexplained variability hampers quantitative analysis based on different patches. We have tried to circumvent this problem in two ways. On one hand, all effects were described thoroughly in individual patches by obtaining complete dose–response data under control and test conditions in the same patch. On the other hand, average responses were computed from patches displaying similar ATP sensitivities under control conditions.

In the presence of inhibiting doses of ATP, activation of K_{ATP} channels by protons was very clear and reproducible from patch to patch as well as within the same patch. This activation was not dependent in any obvious way on the degree of run-down or on the presence of substrates for phosphorylation. As illustrated in Fig. 4*A*, protons were capable of reversing block by ADP as well as by ATP. Because ADP is a weak inhibitor compared with ATP (Spruce *et al.* 1987; Forestier & Vivaudou, 1993*a*), higher doses were required to produce the same level of block. In Fig. 4*A*, a block to about 20% of the control current was achieved with either 0·1 mM ATP or 2 mM ADP. Under both conditions, lowering the pH from 7·1 to 6 caused a similar increase in activity, suggesting that proton effects are dependent more on the level of inhibition than on the particular nucleotide causing that inhibition.

In the majority of patches, the removal of all nucleotides caused nearly maximal activation of K_{ATP} channels. Under these conditions, as P_o was already close to 100%, any further increase in activity by protons could only be marginal and barely discernible (e.g. Fig. 4*A*).

In some patches, for still unknown reasons, channel activity remained sluggish even in the absence of any blocking nucleotide and it could be seen from the noise fluctuations of the current records that P_o was much less than 100%. In such 'sluggish' patches, clear activation by acidification could be observed, as in Fig. 4*B*. This suggests that protons not only interact with nucleotides but also with the unidentified factor which keeps channels from opening when nucleotides are removed. In the following, in

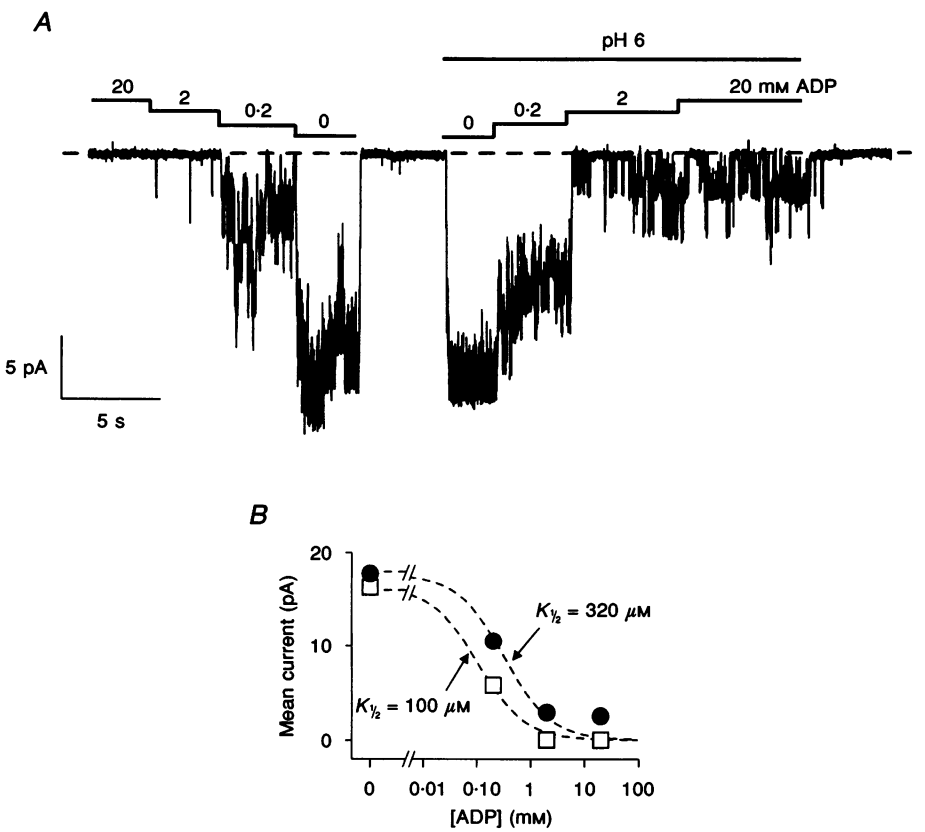

Figure 6. Acidification reduces channel sensitivity to ADP inhibition

A, currents recorded at different concentrations of ADP at neutral and acidic pH. Horizontal bars above the trace indicate the application of ADP at the concentrations shown (without ATP or Mg^{2+}; in the parts of the trace not covered by a bar, a blocking solution of 3 mM ATP and 5 mM Mg^{2+} was applied) and the periods of acidification to pH 6 (pH 7·1 otherwise). f_s, 1 kHz; f_c, 330 Hz. Patch no. 293005. *B*, corresponding plots of the mean current measured at each concentration of ADP *vs.* ADP concentration at pH 7·1 (□) and 6 (●). Dashed lines are best fits of the data points to eqn (1) with the Hill coefficient constrained to 1 and with values of $K_{½}$ of 110 μM at pH 7·1 and 340 μM at pH 6.

order to facilitate interpretation, data from 'sluggish' patches were not included.

Effects of protons on the inhibition by nucleotides of K_{ATP} channels

Davies *et al.* (1992) have shown that the ATP sensitivity of skeletal muscle K_{ATP} channels declines as the pH is lowered from 8 to 6·3. We have extended this observation to include lower pH values as well as to another blocking nucleotide, ADP. Figure 5 shows an example of protocols employed to obtain ATP dose responses at different pH values. This figure shows that the ATP sensitivity of individual patches was reduced by protons in a dose-dependent manner. This effect was observed at proton concentrations higher than 0·1 μM (i.e. pH below neutral). Lower concentrations appeared to have little or no effect because, in several experiments, no obvious change in ATP inhibition was noticed when the pH was changed from 7·1 to 9.

When channels were blocked by ADP instead of ATP, acidification also produced activation due to a lowering of the sensitivity to block by ADP (Fig. 6). Moreover, the range of effective pH values and the shift in sensitivity appeared to be equivalent for ATP and ADP.

Data from several patches were combined in Fig. 7 to show statistically how the ATP dose–response relationship is affected by protons. Patches included had comparable ATP sensitivities ($K_{½}$ at 5–20 μM ATP) under control conditions. The dose–response data were fitted to standard Hill inhibition curves (eqn (1)). As shown in Fig. 7*B*, the Hill coefficients stayed close to 2 with a mean value of 1·8, while $K_{½}$ concentrations increased steeply with decreasing pH. Qualitatively, this behaviour suggests that the pathways for proton activation and ATP inhibition are competitively linked. As more data are presented, we will attempt to translate this hypothesis into concrete quantitative models. In Fig. 7*B*, the dashed lines originate from one such model which will be described later.

Effects of ATP on the activation by protons of K_{ATP} channels

The above observations have shown that proton activation arises from a decrease in nucleotide sensitivity but they have not provided information on the characteristics of this activation, such as the range of effective proton concentrations (or pH values) and the concentration causing 50% activation (or pK value). This was studied by varying the pH over as wide a range as practical under otherwise constant experimental conditions and recording the changes in channel activity in order to build dose–response curves for proton activation as explained in Methods.

Figure 8*A* shows an example of the dependence of K_{ATP} current on pH. In the presence of 0·1 mM ATP, activation began at just below neutral pH and was complete at around pH 5·5 when channels were maximally open. In fact, at very acidic pH, it could often be observed from the noise level of the current record (e.g. Fig. 8*A*) that P_o was close to 1.

The average response of all patches tested in 0·1 mM ATP (Fig. 8*B*) showed a steep pH dependence of channel activity which, when fitted to eqn (2), yielded a pK of 6 and a Hill

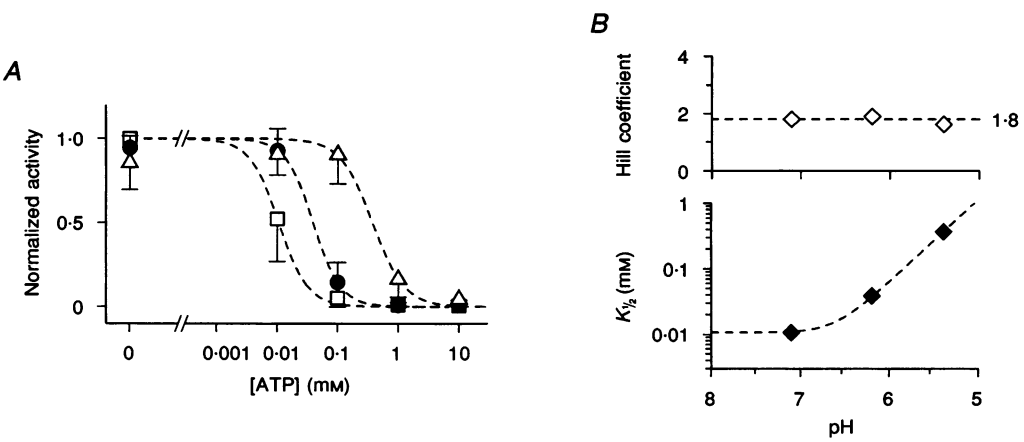

Figure 7. Intracellular protons reduce channel sensitivity to ATP inhibition

A, mean responses to ATP at different pH values computed from data obtained from 6 patches displaying a similar ATP sensitivity at neutral pH. Each plotted point represents the mean ± S.D. of 7–18 measurements obtained using protocols and solutions as in Fig. 6. □, pH 7·1; ●, pH 6·2; △, pH 5·4. Dashed lines are best fits of the data points to eqn (1) with $K_{½}$ and Hill coefficient values, respectively, of 11 μM and 1·8 (pH 7·1), 39 μM and 1·9 (pH 6·2) and 375 μM and 1·6 (pH 5·4). *B*, plots of these Hill coefficients (upper panel, ◇) and $K_{½}$ values (lower panel, ◆) as a function of pH. Dashed lines represent the values of these parameters predicted by the simple simultaneous-binding competitive model described later in the text with K_{ATP} (microscopic ATP dissociation constant), 11 μM; n_{ATP}, 1·8; pK_H, 6·6; and n_H, 2·3.

slope of 2·2. This average behaviour reflected the individual behaviour of each patch well since in seventeen patches the mean pK was 6·0 ± 0·1 and the mean Hill coefficient was 2·3 ± 0·7.

The pK value of a phenomenon is often taken as a rigid characteristic. However, there is no reason to believe that protons should behave differently than any other ligand. We have seen that protons decrease ATP inhibition by a mechanism resembling competition. Conversely, one may ask whether ATP affects proton activation (as implicitly predicted by a competitive model). The answer was obtained by acquiring dose–response data for pH activation in the presence of several different concentrations of ATP. Typical results are illustrated in Fig. 9 in which, in the same patch, it can be seen unequivocally that K_{ATP} channel activation by protons is strongly dependent on the concentration of ATP; as the concentration of ATP is raised, the pH has to be lowered further to reach the same level of activation. Thus ATP effectively shifts the pK of activation towards lower values.

This type of experiment was repeated in a number of patches with various ATP concentrations. Concentrations of ATP within the range 30 μM to 1 mM were used. Concentrations outside this range were of little experimental value because ATP below 30 μM caused too little inhibition even under control conditions and ATP above 1 mM caused too much inhibition even at very acidic pH. Nonetheless, the values tested were sufficient to demonstrate quantitatively the effects of ATP on proton-dependent activation (Fig. 10). The pK of activation decreased progressively by about 1 pH unit, from 6·25 to 5·3, as the ATP concentration was varied from 30 μM to 1 mM (bottom panel of Fig. 10*B*). In parallel, the Hill coefficient appeared to decrease from about 3 to 2, with a mean value of 2·3.

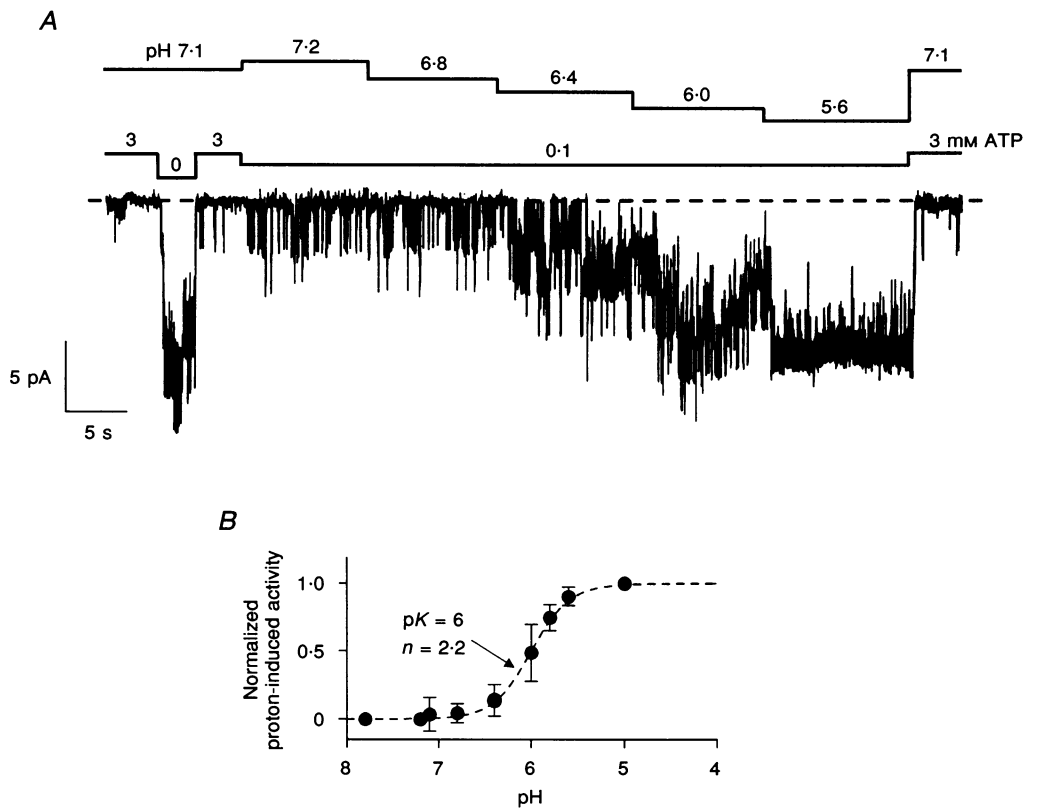

Figure 8. pH dependence of K_{ATP} channel activity in the presence of a partially inhibiting dose of ATP

A, currents recorded at progressively lower pH values in the presence of 0·1 mM ATP. Horizontal bars above the trace indicate the pH and ATP concentrations of the solutions applied. The 3 mM ATP solution contained 5 mM Mg^{2+}, other solutions had no Mg^{2+} added. f_s, 500 Hz; f_c, 200 Hz. Patch no. 321002. The fit to eqn (2) of the plot of channel activity *vs.* pH for this patch yielded pK and Hill coefficient values of 6·2 and 1·8, respectively. *B*, plot of proton-induced channel activity in 0·1 mM ATP *vs.* pH. Proton-induced activity was computed as described in Methods. Each symbol and error bar represents the mean ± S.D. of 3–14 measurements obtained in 14 different patches by application of protocols as in *A*. The dashed line represents the best fit of the data points to eqn (2) with pK and Hill coefficient (n) values of 6·0 and 2·2, respectively.

A competitive model for the interaction between protons and ATP

As a means towards a better functional and structural understanding of K_{ATP} channels, we have tried to build models capable of explaining our results. It must be kept in mind that we are only considering steady-state data and not relaxation or gating kinetics data. We are therefore speaking in terms of binding equilibrium constants rather than time constants.

The individual dose–response data presented above were all fitted with Hill equations (eqns (1) and (2)) as this is the usual way to analyse binding data. This approach constitutes a convenient way of synthesizing the data mathematically but is only a first step towards

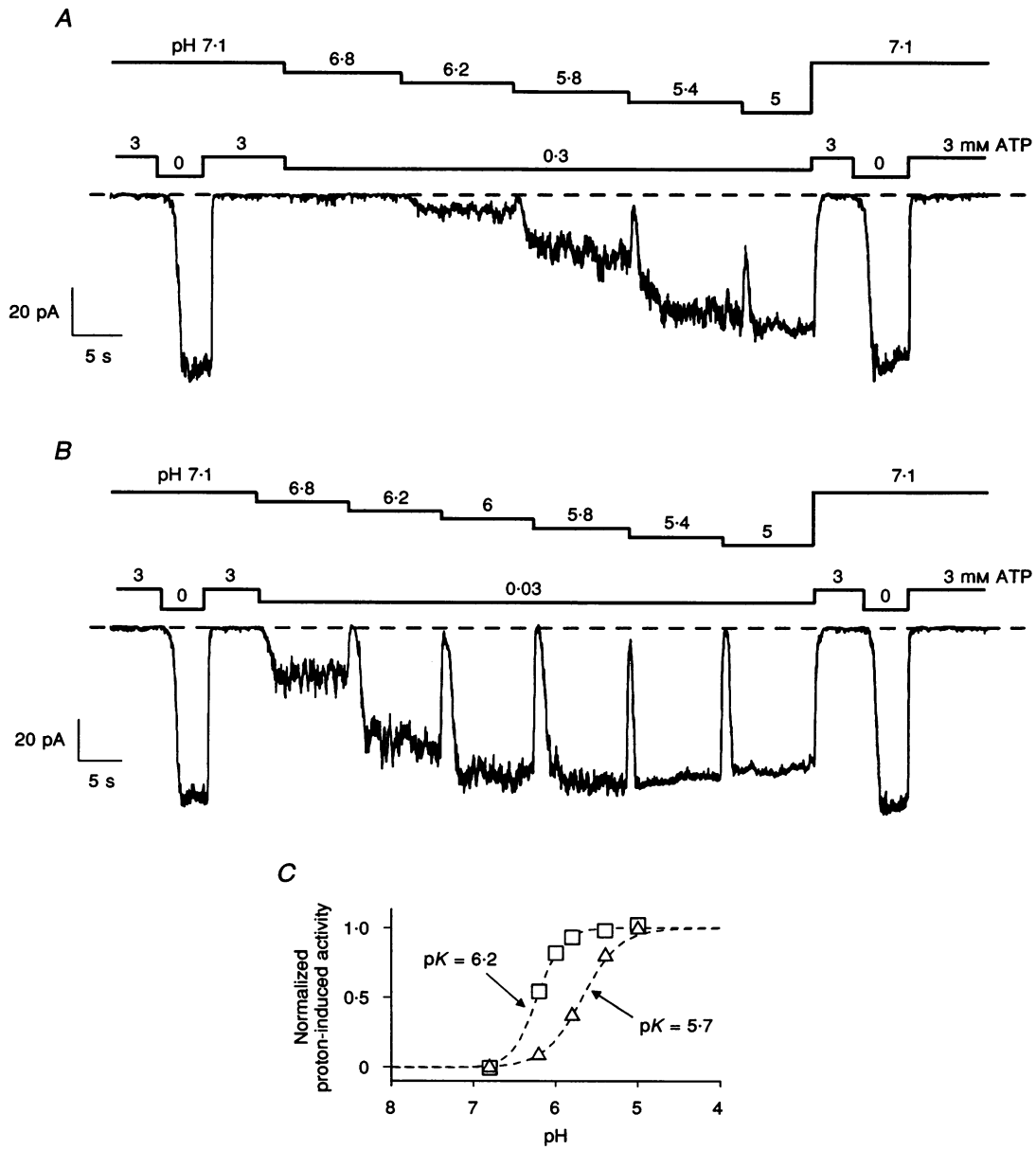

Figure 9. Intracellular ATP shifts the pH dependence of K_{ATP} channel activity

A, currents recorded at progressively lower pH values in the presence of 0·3 mM ATP. Horizontal bars above the trace indicate the pH and ATP concentrations of the solutions applied. The 3 mM ATP solution contained 5 mM Mg^{2+}, other solutions had no Mg^{2+} added. f_s, 110 Hz; f_c, 30 Hz. Patch no. 3C1404. *B*, same protocol and conditions as in *A* but in the presence of 0·03 mM ATP. This trace was recorded 10 s after the trace in *A*. *C*, corresponding plots of the proton-induced channel activity *vs.* pH in the presence of either 0·3 mM ATP (△, *A*) or 0·03 mM ATP (□, *B*). Dashed lines are best fits of the data points to eqn (2) with p*K* and Hill coefficient values, respectively, of 5·7 and 1·9 (0·3 mM ATP) and 6·2 and 2·9 (0·03 mM ATP).

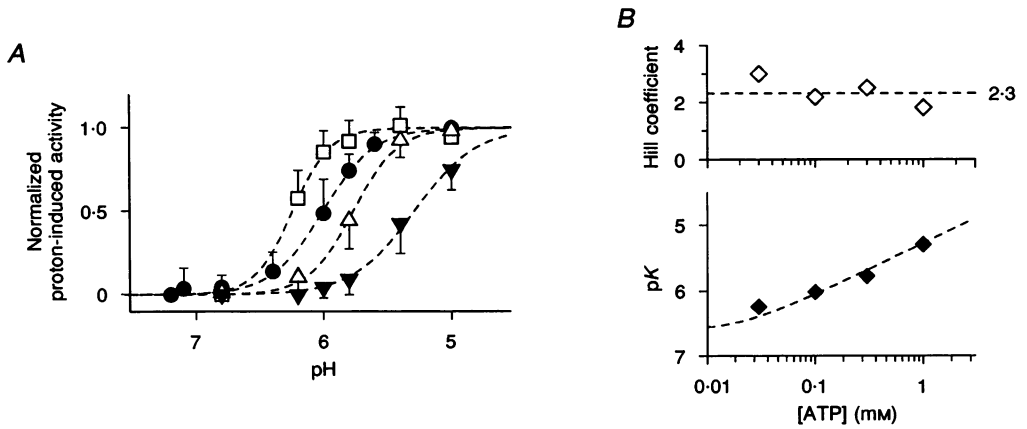

Figure 10. Intracellular ATP reduces channel sensitivity to activation by protons

A, mean responses to pH at different ATP concentrations compiled from the responses of 24 patches. Each plotted point represents the mean ± S.D. of 3–17 measurements obtained using the protocols and solutions of Figs 8 and 9. Dashed lines are best fits of the data points to eqn (2) with pK and Hill coefficient values, respectively, of 6·25 and 3·0 (0·03 mM ATP; □), 6·0 and 2·2 (0·1 mM ATP; ●), 5·8 and 2·5 (0·3 mM ATP; △) and 5·3 and 1·8 (1 mM ATP; ▼). *B*, plots of these Hill coefficient (upper panel; ◇) and pK (lower panel; ◆) values as a function of ATP. Dashed lines represent the values of these parameters predicted by the simple simultaneous-binding competitive model described in the text with values: K_{ATP}, 20 μM; n_{ATP}, 1·8; pK_H, 6·6; and n_H, 2·3.

understanding the actual physical mechanism. Taking, as an hypothesis, that the channel state, open or closed, is directly related to ligand occupancy, the opening action of protons at a given concentration of ATP may be approximated by the right-hand reaction of theoretical scheme 1 of Fig. 11 in which the simultaneous, i.e. fully co-operative, binding of n_H protons (not necessarily an integer number in this mathematical model) causes the channel to open. This scheme corresponds to eqn (1) where the Hill coefficient, n, equals n_H. Similarly the closing action of ATP is represented by the left-hand reaction of scheme 1 of Fig. 11 which conforms with eqn (2). The simplest scheme that could account for the observed competitive behaviour between protons and ATP is the full scheme 1 of Fig. 11.

The four parameters of this model were adjusted until predictions agreed with the data of Figs 7 and 10. An almost perfect match, as judged by eye, between the model and the observed pH dependence of ATP inhibition (Fig. 7) was reached with values of n_H of 2·3, pK_H of 6·6, n_{ATP} of 1·8 and K_{ATP} (microscopic dissociation constant for ATP) of

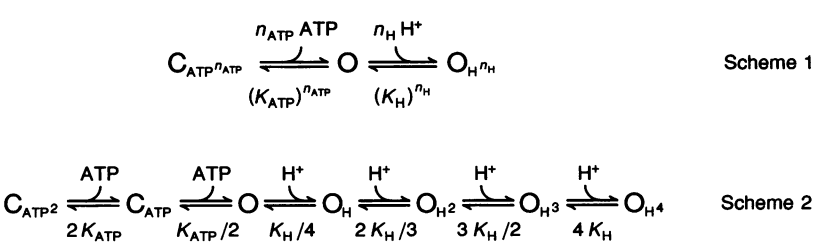

Figure 11. Reaction schemes considered to explain isolated and combined effects of protons and ATP on open probability of the K_{ATP} channel

The symbols O and C refer to the channel being open and closed, respectively. The apparent dissociation constants for each equilibrium are indicated below the reaction arrows. Scheme 1, theoretical Hill reaction for stabilization of the open state by simultaneous binding of n_H protons corresponding to eqn (1) and closing of the channel by simultaneous binding of n_{ATP} ATP molecules corresponding to eqn (2). Scheme 2, hypothetical equilibrium reaction scheme for a channel having n_H (here 4) equivalent proton sites linked to an open state and n_{ATP} (here 2) equivalent ATP sites linked to a closed state. Microscopic dissociation constants for each species of sites are K_{ATP} and K_H and the indicated apparent dissociation constants for each successive binding step are related to these microscopic constants by a factor which takes into account all the possible ligand occupancy combinations associated with a given state in the diagram (Monod, Wyman & Changeux, 1965).

11 μM. The dashed lines in Fig. 7*B* represent predictions based on these values. The best fit to the observed ATP dependence of proton activation (Fig. 10) led to identical values of n_H, pK_H and n_{ATP} but K_{ATP} had to be changed to 20 μM. Again, the dashed lines in Fig. 10*B* represent predictions based on these latter values. Given the high variability of K_{ATP} channel sensitivity to ATP, it is not surprising that the model K_{ATP} value had to be adjusted to fit different sets of experiments. However the difference between the two values of K_{ATP} is small and an adequate although not perfect prediction of all experimental data could be reached by choosing an intermediary K_{ATP} value of 15 μM with additional parameters as previously.

Thus, our observations appear to be theoretically consistent with a competitive mechanism. Starting from the ideal competitive scheme 1, we have investigated how proton and ATP binding sites could be linked together to account for the data. Since both proton activation dose–response curves and ATP inhibition dose–response curves had Hill slopes greater than 1, it is reasonable to admit that, for each ligand, there are at least two sites and that these sites are co-operatively coupled in a positive manner. We therefore assumed n_{ATP} sites for ATP and n_H sites for protons (both integer numbers). For simplicity, all sites were considered equivalent with the same microscopic dissociation constants, K_{ATP} for ATP and K_H ($= 10^{-pK_H}$) for protons. Furthermore, a degree of co-operativity between each site was introduced by assuming that each ligand binds only to one conformation of the channel and that the channel remains in that conformation whenever one or more ligand molecules are bound. For protons, that conformation would correspond to an open state of the channel and for ATP to a closed state. An example of such a system with values of n_{ATP} and n_H of 2 and 4, respectively, is represented as scheme 2 in Fig. 11. This scheme, like scheme 1, has only four free parameters and predictions can be readily evaluated using formulations similar to those used by Monod *et al.* 1965. Thus, if X designates the ligand-free channel, X_H the channel with one or more protons bound and X_{ATP} the channel with one or more ATP bound then:

$$\alpha = \frac{[X_H]}{[X]} = \left(1 + \frac{[H]}{K_H}\right)^{n_H} - 1$$

and

$$\beta = \frac{[X_{ATP}]}{[X]} = \left(1 + \frac{[ATP]}{K_{ATP}}\right)^{n_{ATP}} - 1. \quad (8)$$

Using these relations and assuming the channel is closed in all ATP-bound states and open otherwise, it is straightforward to calculate open probability which is simply:

$$P_o = \frac{1 + \alpha}{1 + \alpha + \beta}. \quad (9)$$

Varying parameters to adjust predictions to the experimental dose–response curves of Figs 7*A* and 10*A*, we determined that: (1) the only acceptable value for n_{ATP} was 2, (2) fits deemed acceptable required n_H to be either 3 or 4, and (3) as before, best fits to each set of data required slightly different values of K_{ATP}.

As model predictions were no better using an n_H value of 3 rather than 4, we preferred, for reasons of symmetry, to select the latter value as a basis for discussion. The presence of four protonation sites is also more seductive given the proposed tetrameric structure of most cloned K^+-selective channels (e.g. Mackinnon, 1991). For the model with an n_H value of 4, best parameters were pK_H of 6·0, n_{ATP} of 2, and K_{ATP} of either 36 μM for optimal fit to the pH dependence of ATP inhibition (Fig. 7*A*) or 21 μM for the ATP

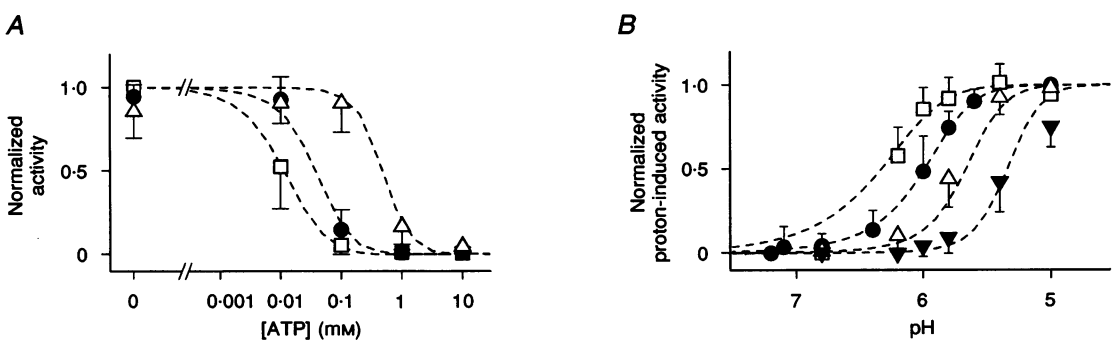

Figure 12. Model predictions match all experimental observations on the isolated and combined effects of protons and ATP on K_{ATP} channels

A, pH dependence of ATP inhibition. Experimental points represented by symbols are redrawn from Fig. 7*A*. □, pH 7·1; ●, pH 6·2; △, pH 5·4. Dashed lines are predictions from scheme 2 of Fig. 11 with values: n_H, 4; pK_H, 6·0; n_{ATP}, 2; and K_{ATP}, 36 μM. *B*, ATP dependence of proton activation. Experimental points represented by symbols are redrawn from Fig. 10*A*. □, 0·03 mM ATP; ●, 0·1 mM ATP; △, 0·3 mM ATP; ▼, 1 mM ATP. Dashed lines are predictions from the model with values: n_H, 4; pK_H, 6·0; n_{ATP}, 2; and K_{ATP}, 21 μM.

dependence of proton activation (Fig. 10*A*). The predicted data together with the experimental dose–response data are shown in Fig. 12. This figure demonstrates that such a model is capable of satisfactorily predicting channel behaviour. Of course, one can always imagine more complex models which would be adequate but we were not able to find any simpler yet realistic model which could account for the experimental observations.

DISCUSSION

In this paper, we have examined in detail the effects of protons on the two most basic properties of K_{ATP} channels: ion conduction and inhibition by adenine nucleotides. In skeletal muscle, protons have other more complex effects on the action of pharmacological K^+ channel openers (Forestier, Depresle & Vivaudou, 1993), which we shall not discuss here.

Protons and Mg^{2+} ions reduce inward open-channel currents

Inward unit current reduction by cytoplasmic protons can be explained by at least three different types of mechanism: direct pore block, induction of lower conductance states and electrostatic effects. In the first hypothesis, protons would directly plug the conduction pathway and, by shuttling in and out rapidly, would cause a smooth dose-dependent reduction in unitary current at the limited recording bandwidth used here. As pH is lowered, this reduction would proceed along a Langmuir adsorption isotherm until current is null. The observed noise level might also be affected and, as protonation sites are located within the transmembrane electrical field, the effect would be voltage dependent. This mechanism appears unlikely here since none of these predictions were verified by our observations.

The second mechanism has been demonstrated in the case of the dihydropyridine-sensitive Ca^{2+} channel where external protonation causes a voltage-independent discrete reduction in conductance probably via a conformational change (Pietrobon, Prod'hom & Hess, 1989). Such a mechanism would be more consistent than the previous one with the observed unit current *vs.* pH relationship (Fig. 3*A*). Indeed, Fan *et al.* (1993) have shown that single cardiac K_{ATP} channels exhibit inward subconductance levels under conditions of strong intracellular acidification ($pH < 6$). These sublevels remained infrequent compared with the main highest level. Moreover, acidification also caused a clear, gradual reduction in the amplitude of all levels. This last observation is much like ours. However, under similar filtering conditions, we have seen no evidence for proton- or Mg^{2+}-induced subconductance states (e.g. see traces in Fig. 2), although these events could be much faster under our conditions. Nonetheless, it remains difficult to imagine how protons acting through allosteric interactions would cause a horizontal shift of the current–voltage relationship as in Fig. 2.

We have therefore considered a third model in which protons would affect the electrical field profile of the K_{ATP} channel pore by binding to negatively-charged sites located near the cytoplasmic entrance of the pore. Our model is partly based on that proposed by Mackinnon *et al.* (1989) who were confronted with similar data concerning the effects of cations on single K_{Ca} channel currents. Their model assumed that cations neutralized surface charges by screening only. In the case of protons, the screening effect is all but negligible at workable pH values because of their low concentration (Gilbert & Ehrenstein, 1984). We have therefore added the possibility of neutralization of surface charges by direct binding. Using the Gouy–Chapman–Stern theory with a density of about 0·1 charges nm^{-2}, a binding pK of 6·25, and a binding constant for Mg^{2+} of 30 mM, this model predicted the dependence of inward current amplitude on both protons and Mg^{2+} ions well. A surface charge density of 0·1 negative charges nm^{-2} is within the range of previously reported values for the intracellular end of cationic channels (e.g. Gilbert & Ehrenstein, 1984; Kuo & Hess, 1992). The pK value of 6·25 could point to histidine residues although we know how hazardous it is to extrapolate protein characteristics from properties of single amino acids.

The fact that parameters can be found for which the surface charge model can predict the experimental results does not demonstrate unequivocally the validity of this model. Using more extensive arguments, such a mechanism has been shown to apply to another K^+ channel, the large Ca^{2+}-activated K^+ channel (Mackinnon *et al.* 1989). Unlike K_{Ca} channels, K_{ATP} channels are not patently gated by voltage and, as a consequence, we cannot monitor voltage-dependent parameters to test for changes in the transmembrane electrical field as was done by Mackinnon *et al.* (1989). Nonetheless, surface charge neutralization by protonation explains the effects of both protons and Mg^{2+} better than either direct block or indirect allosteric block.

Competitive interaction between protons and nucleotides regulates gating of K_{ATP} channels

If protons impair ion conduction through skeletal muscle K_{ATP} channels, their most visible and physiologically relevant action is the augmentation of open probability first described by Davies (1990). This phenomenon was analysed by Davies *et al.* (1992) who found that acidification shifted the channel activity *vs.* ATP concentration curve towards higher ATP concentrations. A competitive model was proposed with two protonation sites linked to the open state and one ATP site linked to the closed state. This model was found to be compatible with the observed pH dependence of the ATP concentration for half-maximal inhibition.

In this work, we have explored this mechanism further using more substantial experimental data on the interaction between protons and nucleotides. We have found that, just as protons reduced the sensitivity of the K_{ATP} channels to ATP, ATP reduced the sensitivity of these channels to protons. Moreover, protons had very similar effects when ADP instead of ATP was used to block the channel. This finding reinforces the hypothesis that these nucleotides share and compete for the same inhibitory binding sites (Vivaudou *et al.* 1991). In our hands, protons could also potentiate K_{ATP} channel activity in the absence of nucleotides in those 'sluggish' patches in which channel activity remained low under high-pH nucleotide-free control conditions. This observation could not be analysed in great detail because the degree of 'sluggishness' was unpredictable and very variable. Run-down, which is also difficult to study for the same reasons, did not seem to be linked to 'sluggishness'. It may be that 'sluggishness' is controlled by an unknown blocking factor of variable activity from patch to patch. Since protons could therefore reverse this inhibition as well as the inhibition by nucleotides, one could speculate that this factor causes channel inhibition by the same mechanism and possibly via the same binding sites as nucleotides. A better understanding, and consequently better control, of this process will have to await further experiments. In the meantime, sluggish patches, fortunately a minority, were avoided in our analysis of proton–nucleotide interactions.

In terms of mechanism, our results support the hypothesis of Davies *et al.* (1992) of an apparent competition between protons and ATP but lead to more complex models. The simplest model which could account for the data involves four allosterically coupled protonation sites which stabilize an open conformation of the channel and two allosterically coupled ATP sites which stabilize a closed conformation. Such a model permits the prediction of not only pH-induced changes in ATP sensitivity but also ATP-induced changes in pH sensitivity as well as the steepness of the relationships between channel activity and both pH and ATP.

Relative inhibitory potencies of the different ionized forms of ATP

Nucleotides are able to bind protons and metals to various extents and will therefore exist in solution under different ionic forms which may have distinct effects on K_{ATP} channel activity. We already know that, in our preparation, ATP and ADP lose much of their inhibitory potency when bound to Mg^{2+} (Vivaudou *et al.* 1991; Forestier & Vivaudou, 1993*a*). It has also been suggested that, in pancreatic β-cells, the potency of inhibition could be augmented by the valency of nucleotide anions (Ashcroft & Kakei, 1989).

Since the concentrations of these ionic forms change with pH, one may wonder to what extent changes in the relative proportion of the ATP species could have affected our observations. At one extreme, could indirect chemical interactions account for all effects? Activation by protons was observed with and without Mg^{2+} and cannot be explained by proton-induced shifts in the balance between Mg^{2+}-free and Mg^{2+}-bound nucleotides.

In the absence of Mg^{2+}, there still remain three main ATP species, ATP^{4-}, $ATPH^{3-}$ and $ATPK^{3-}$ and minor species such as $ATPH^{2-}$ which remain negligible under our experimental conditions. Because the pK for ATP is about 6·5 (Dawson, Elliott, Elliott & Jones, 1986), the relative amounts of these three species do change significantly over the pH range that we have examined. As pH is lowered from 8 to 5, ATP^{4-} and $ATPK^{3-}$ decrease while $ATPH^{3-}$ increases. We have evaluated and numerically simulated a number of schemes by which these variations could produce the pH effects observed, independent of any direct effect of protons on the channel. One plausible scheme would be that only ATP^{4-} is capable of blocking the channel. In that case, assuming gating model 2 of Fig. 11, it is possible to predict our results, at least qualitatively, in particular, the shift by protons of the ATP dose–response curve as well as the shift by ATP of the proton dose–response curve. Nevertheless, the scheme fails in the presence of millimolar concentrations of Mg^{2+}; then, ATP^{4-} remains low and varies little at pH values above 5, and yet we and others (Davies, 1990) have seen clear activation of K_{ATP} channels by protons in 1–5 mM Mg^{2+}. However, if one further postulates that $ATPH^{3-}$ competes with ATP^{4-} but does not block the channel, it is possible to predict some degree of activation by protons with and without Mg^{2+} but at the expense of more adjustable parameters and a poor quantitative agreement with the experimental results.

Therefore, a contribution of chemical interactions to our observations cannot be discarded completely but, to be significant, such a contribution would require a complex mechanism that the available evidence is insufficient to either prove or disprove. Consequently, without further evidence, we feel that it is not justified to assume any significant difference in the inhibitory potencies of the different Mg^{2+}-free forms of ATP.

Structural implications

Our proposed model is based only on steady-state ATP and pH dependence of K_{ATP} channels. The integration of kinetics data would certainly require building more complex models, a rather unrewarding exercise given the lack of structural information. Considering only ATP inhibition, Nichols, Lederer & Cannell (1991) did propose a scheme compatible with steady-state and kinetic responses of cardiac K_{ATP} channels. This scheme assumed two identical pairs of sequential ATP binding sites. Our data on steady-state ATP dependence of channel activity are in fact greatly similar to that obtained in heart (e.g. Lederer & Nichols, 1989) and would certainly be compatible with such a scheme. This limited data, however, did not warrant

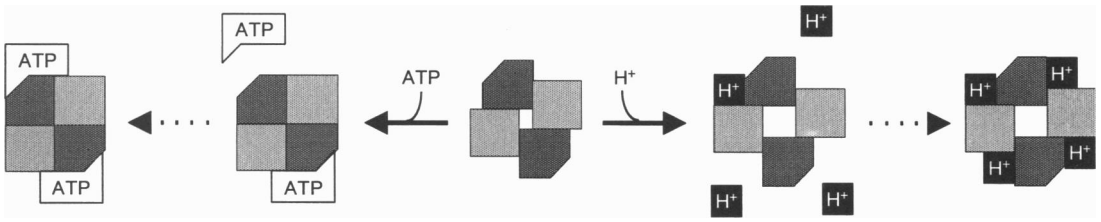

Figure 13. A hypothetical structural model of a tetrameric K_{ATP} channel
This model would conform to steady-state reaction scheme 2 of Fig. 11. The channel complex would possess 2 concerted ATP binding sites stabilizing a closed conformation and 4 concerted protonation sites stabilizing an open conformation. The channel would have 2 types of subunit arranged in pairs and subunit motion would be constrained to maintain the channel axial symmetry.

anything more complex than two identical ATP sites coupled to the closed configuration. Assuming that K_{ATP} channels adopt a tetrameric structure, as proposed for other K^+ channels (Mackinnon, 1991), one may imagine an allosteric model of a channel (Fig. 13) with two pairs of subunits and distinct proton and nucleotide binding sites. In the absence of ligands, the channel would reside in open and closed conformations in which proton and nucleotide binding sites would be accessible. Binding of a proton to any of the protonation sites would constrain the channel to an open conformation, which would preserve binding sites for protons but not for nucleotides. Conversely, binding of a nucleotide would stabilize a closed conformation accessible exclusively to nucleotides. Previous (Vivaudou *et al.* 1991; Forestier & Vivaudou, 1993*a*) and present evidence suggest that the nucleotide binding sites have a greater affinity for ATP than ADP, that both nucleotides are less active when complexed with Mg^{2+}, and that the affinity of all Mg^{2+}-free forms of ATP are equivalent.

Obviously, since our data yielded information only on coupled sites, other models with more sites (e.g. four protonation sites and two ATP sites per subunit and four uncoupled subunits) are possible. This model, like that of Nichols *et al.* (1991) assumes a tetrameric structure but two types of subunit. The source of this asymmetry, either structural or functional, remains to be identified.

Our interpretation of the effects of protons on conduction argues for the location of protonation sites near the intracellular entrance of the K_{ATP} channel conduction pathway. We postulate that these 'surface charge' sites are different from the above 'gating' sites. Indeed, proton-dependent K_{ATP} conductance changes similar to those we measured have been observed in other tissues, like pancreas (Proks *et al.* 1994) and heart (Cuevas *et al.* 1991; Koyano *et al.* 1993). However, effects on gating in these tissues did not resemble, in magnitude or in sign, the effects in skeletal muscle. In the pH range that we have used, intracellular protons decreased activity in guinea-pig ($pH < 6$ only; Koyano *et al.* 1993) and rabbit (Fan & Makielski, 1993) ventricular myocytes, and rat (Misler, Gillis & Tabcharani, 1989) and mouse (Proks *et al.* 1994) pancreatic β-cells. They increased activity somewhat in rat (Lederer & Nichols, 1989), cat (Cuevas *et al.* 1991), guinea-pig ($pH > 6$ only; Koyano *et al.* 1993) and rabbit (Fan & Makielski, 1993) ventricular myocytes. Since the same effect on conductance can be accompanied by very different effects on P_o depending on the preparation, one may assume that these two effects are independent and can be studied separately as we have done. Moreover, this suggests that the domain of K_{ATP} channels with which protons interact to modify inward conductance, i.e. the intracellular entrance of the channel pore, is well conserved among species and tissues. On the other hand, the channel region or subunit involved in proton-induced gating changes would be more variable among tissues. This region could be a tissue-specific regulatory domain endowed with protonation sites and linked to nucleotide regulation which is also very variable among cell types (Ashcroft & Ashcroft, 1990).

Allard, B. & Lazdunski, M. (1992). Nucleotide diphosphates activate the ATP-sensitive potassium channel in mouse skeletal muscle. *Pflügers Archiv* **422**, 185–192.

Ashcroft, S. J. H. & Ashcroft, F. M. (1990). Properties and functions of ATP-sensitive K-channels. *Cellular Signalling* **2**, 197–214.

Ashcroft, F. M. & Kakei, M. (1989). ATP-sensitive K^+ channels in pancreatic β-cells: modulation by ATP and Mg^{2+} ions. *Journal of Physiology* **416**, 349–367.

Cannell, M. B. & Nichols, C. G. (1991). Effects of pipette geometry on the time course of solution change in patch-clamp experiments. *Biophysical Journal* **60**, 1156–1163.

Cuevas, J., Bassett, A. L., Cameron, J. S., Furukawa, T., Myerburg, R. J. & Kimura, S. (1991). Effect of H^+ on ATP-regulated K^+ channels in feline ventricular myocytes. *American Journal of Physiology* **261**, H755–761.

Davies, N. W. (1990). Modulation of ATP-sensitive K^+ channels in skeletal muscle by intracellular protons. *Nature* **343**, 375–377.

Davies, N. W., Standen, N. B. & Stanfield, P. R. (1992). The effect of intracellular pH on ATP-dependent potassium channels of frog skeletal muscle. *Journal of Physiology* **445**, 549–568.

DAWSON, R. M. C., ELLIOTT, D. C., ELLIOTT, W. H. & JONES, K. M. (1986). *Data for Biochemical Research*, 3rd edn, Oxford University Press, Oxford, UK.

FAN, Z., FURUKAWA, T., SAWANOBORI, T., MAKIELSKI, J. C. & HIRAOKA, M. (1993). Cytoplasmic acidosis induces multiple conductance states in ATP-sensitive potassium channels of cardiac myocytes. *Journal of Membrane Biology* **136**, 169–179.

FAN, Z. & MAKIELSKI, J. C. (1993). Intracellular H^+ and Ca^{2+} modulation of trypsin-modified ATP-sensitive K^+ channels in rabbit ventricular myocytes. *Circulation Research* **72**, 715–722.

FINDLAY, I. (1987). The effects of magnesium upon adenosine triphosphate-sensitive potassium channels in a rat insulin-secreting cell line. *Journal of Physiology* **391**, 611–629.

FINDLAY, I. & FAIVRE, J. F. (1991). ATP-sensitive K channels in heart muscle: spare channels. *FEBS Letters* **279**, 95–97.

FORESTIER, C., DEPRESLE, Y. & VIVAUDOU, M. (1993). Intracellular protons control the affinity of skeletal muscle ATP-sensitive K^+ channels for potassium-channel-openers. *FEBS Letters* **325**, 276–280.

FORESTIER, C. & VIVAUDOU, M. (1993*a*). Modulation by Mg^{2+} and ADP of ATP-sensitive potassium channels in frog skeletal muscle. *Journal of Membrane Biology* **132**, 87–94.

FORESTIER, C. & VIVAUDOU, M. B. (1993*b*). Activation of skeletal muscle K-ATP channels by protons and lemakalim: a comparative study. *Biophysical Journal* **64**, A316.

GILBERT, D. L. & EHRENSTEIN, G. (1984). Membrane surface charge. *Current Topics in Membranes and Transport* **22**, 407–421.

HAMILL, O. P., MARTY, A., NEHER, E., SAKMANN, B. & SIGWORTH, F. J. (1981). Improved patch-clamp techniques for high-resolution current recordings from cells and cell-free membrane patches. *Pflügers Archiv* **391**, 85–100.

HILLE, B. (1992). *Ionic Channels of Excitable Membranes*, 2nd edn, Sinauer Associates, Sunderland, MA, USA.

HORIE, M., IRISAWA, H. & NOMA, A. (1987). Voltage-dependent magnesium block of adenosine-triphosphate-sensitive potassium channel in guinea-pig ventricular cells. *Journal of Physiology* **387**, 251–272.

KOYANO, T., KAKEI, M., NAKASHIMA, H., YOSHINAGA, M., MATSUOKA, T. & TANAKA, H. (1993). ATP-regulated K^+ channels are modulated by intracellular H^+ in guinea-pig ventricular cells. *Journal of Physiology* **463**, 747–766.

KUO, C.-C. & HESS, P. (1992). A functional view of the entrances of L-type Ca^{2+} channels – estimates of the size and surface potential at the pore mouths. *Neuron* **9**, 515–526.

LEDERER, W. J. & NICHOLS, C. G. (1989). Nucleotide modulation of the activity of rat heart ATP-sensitive K^+ channels in isolated membrane patches. *Journal of Physiology* **419**, 193–211.

MACKINNON, R. (1991). Determination of the subunit stoichiometry of a voltage-activated potassium channel. *Nature* **350**, 232–235.

MACKINNON, R., LATORRE, R. & MILLER, C. (1989). Role of surface electrostatics in the operation of a high-conductance Ca^{2+}-activated K^+ channel. *Biochemistry* **28**, 8092–8099.

MCLAUGHLIN, S. (1977). Electrostatic potentials at membrane–solution interfaces. *Current Topics in Membranes and Transport* **9**, 71–144.

MCLAUGHLIN, S., MULRINE, N., GRESALFI, T., VAIO, G. & MCLAUGHLIN, A. (1981). Adsorption of divalent cations to bilayer membranes containing phosphatidylserine. *Journal of General Physiology* **77**, 445–473.

MCLAUGHLIN, S. G. A., SZABO, G. & EISENMAN, G. (1971). Divalent ions and the surface potential of charged phospholipid membranes. *Journal of General Physiology* **58**, 667–687.

MISLER, S., GILLIS, K. & TABCHARANI, J. (1989). Modulation of gating of a metabolically regulated, ATP-dependent K^+ channel by intracellular pH in B cells of the pancreatic islet. *Journal of Membrane Biology* **109**, 135–143.

MONOD, J., WYMAN, J. & CHANGEUX, J. P. (1965). On the nature of allosteric transitions: a plausible model. *Journal of Molecular Biology* **12**, 88–118.

NICHOLS, C. G., LEDERER, W. J. & CANNELL, M. B. (1991). ATP dependence of K_{ATP} channel kinetics in isolated membrane patches from rat ventricle. *Biophysical Journal* **60**, 1164–1177.

PIETROBON, D., PROD'HOM, B. & HESS, P. (1989). Interactions of protons with single open L-type calcium channels – pH dependence of proton-induced current fluctuations with Cs^+, K^+, and Na^+ as permeant ions. *Journal of General Physiology* **94**, 1–21.

PROKS, P., TAKANO, M. & ASHCROFT, F. M. (1994). Effects of intracellular pH on ATP-sensitive K^+ channels in mouse pancreatic β-cells. *Journal of Physiology* **475**, 33–44.

SPRUCE, A. E., STANDEN, N. B. & STANFIELD, P. R. (1987). Studies of the unitary properties of adenosine-5′-triphosphate-regulated potassium channels of frog skeletal muscle. *Journal of Physiology* **382**, 213–236.

VIVAUDOU, M. B., ARNOULT, C. & VILLAZ, M. (1991). Skeletal muscle ATP-sensitive potassium channels recorded from sarcolemmal blebs of split fibers: ATP inhibition is reduced by magnesium and ADP. *Journal of Membrane Biology* **122**, 165–175.

WILSON, D. L., MORIMOTO, K., TSUDA, Y. & BROWN, A. M. (1983). Interaction between calcium ions and surface charges as it relates to calcium currents. *Journal of Membrane Biology* **72**, 117–130.

YELLEN, G. (1982). Single Ca-activated nonselective cation channels in neuroblastoma. *Nature* **296**, 357–359.

Author's present address

C. Forestier: CEA, DPVE-SBC, 13108 St Paul-lez-Durance, France.

Received 29 September 1994; accepted 6 February 1995.